



# Detection and Location of Partial Discharge on a Power Transformer by Applying Acoustic and UHF Sensors

Raza Mehrjou<sup>1</sup> and Seyed Mohammad Hassan Hosseini<sup>1,\*</sup>

## ARTICLE INFO

### Article history:

Received: 30 July 2023

Revised: 14 February 2024

Accepted: 11 March 2024

### Keywords:

Acoustic sensors

Partial discharge (PD)

Power transformer

UHF antennas

## ABSTRACT

This paper presented a combined method for detecting and locating partial discharge in power transformers applying only one acoustic and UHF sensor. Transformers and sensors simulated in the COMSOL MULTIPHYSICS 5.2a are based on the real model. A practical example is used to explain this method. Transformers and sensors based on the model are simulated in COMSOL MULTIPHYSICS 5.2a, for this study used a 20 kV / 0.4 kV -1MVA transformer, an R30 $\alpha$  acoustic sensor, and a regular *Ultra high frequency* (UHF) probe. Simulated transformer Includes transformer tank, core, coils, and transformer oil. The variable capacity cylinder simulates the partial discharge (PD) source. The simulated transformer then, by placing a simulated PD source on all of the transformers and taking sensor responses. This data imports to MATLAB database (pattern database); this database is part of the designed application for MATLAB to analyze the direct acoustic and UHF sensor signal from the oscilloscope. The analysis data is a comparison between input data (sensor signal) and pattern database (which was created by simulation data) using pattern recognition by the designed algorithm. Next stage any actual Signal from sensor and transformer similar to sensor and transformer used in the simulation can be detected PD location, source charge, and any data was created in the pattern database. For Verification, this method tested on a real sample in the laboratory. Specifications of the equipment used in the test are identical with the simulation results.

## 1. INTRODUCTION

Insulation systems are one of the most critical components of power systems. Moreover, PD is an essential factor in the gradual degradation of insulation. The negative impact of partial discharge in the decline of electrical insulation's useful life has been studied for years [1].

For this reason, partial discharge's continuous monitoring and the health status of insulation in power transformers are essential as one of the most critical steps in maintaining the stability of power systems. Partial discharge Non-destructive testing due non-damaged to insulation structure is widely used in the health state monitoring of high voltage insulator and especially power transformer insulation [2]. The use of this method has begun since the 1970s. The process for continuous monitoring of electrical insulation found full acceptance when the research has identified electrical insulation's health state as one of the essential factors in maintaining and improving the stability of power systems [3]. Non-destructive methods divide into two categories: conventional and non-conventional. The purposes of using acoustic and UHF sensors are the most crucial non-conventional detection methods for PD

activities [4]. These methods have been slowly taken into account in recent years due to their many advantages and abilities. In the last two decades, many studies have been carried out to improve the old methods or to provide a new method for detecting partial discharge in the transformer to the use of an acoustic and electromagnetic (UHF) sensor [5]. These two methods are sometimes combined with the conventional method of partial discharge's electrical measuring, which is the result of a relatively successful method for monitoring the PD in the transformer. The methods that are commonly used for PD detection and location are online, in practice, using these methods involves three problems of cost, accuracy, and complexity at launch. According to this study is to provide a low-cost way by maintaining accuracy. This method applies to all transformers at low cost. In the same survey, the result of the simultaneous use of both acoustic and electromagnetic sensor is not so acceptable and in the low-cost method is relatively low accuracy [6-8].

This work has attempted to solve the problem with a single sensor by a new method. The transformer and the cavity's PD generator are simulated on COMSOL

<sup>1</sup>Department of Electrical Engineering, South Tehran Branch, Islamic Azad University, Tehran, Iran.

\*Corresponding author: Seyed Mohammad Hassan Hosseini; E-mail: Smhh110@azad.ac.ir.

MULTIPHYSICS 5.2a. Then acoustic and UHF sensors are simulated based on an actual model with real values on Simulation Workplace. Then by entering the source of PD in the simulation, activate the simulation. Next, by moving the discharge source at the point-to-point simulated transformer's environment and recording the sensor response for all locations and sizes of the PD in a created database on MATLAB by a pattern recognition using MATLAB between sensor data and Comsol output can type, size and location of PD to be detected.

## 2. SIMULATE AND MATLAB INTERFACE

For the simulation stage, the transformer, sensors, and the PD source (cavity) have been fully modeled. All dimensions are in millimeters and measurement units in the SI system. Used data from the test sample at all stages of the simulation.

### 2.1. Geometry

The first simulation stage of the desired transformer is the creation of the structural geometry of the model. On mathematical research, the choice of modeling numerical equations and then the creation of the structure and production of model space are essential [9, 10]. But in the software used in this study, by introducing the exact geometric characteristics of the model and selecting the dependencies of the geometry of the model with the physics used in the simulation of the vector and numerical space required to simulate using their own software equations and methods It is based on the repetition of the software. This feature allows us to easily create a model without regard to a large number of equations or the need for frequent misconceptions in the structure of the geometry of the model. Some transformer components sizes are extracted from the catalog, and the rest is obtained by inquiries from the manufacturer's lab. To model the cavity in which partial discharge occurs. A cavity can be modeled as a cylinder which changes its discharge capacity by changing its shape. The size data in the table. The propagation model in the tank space of the transformer is checked. Also, the sensors are aligned in the same direction [11, 12]. Therefore, the bushing modeling and the relays connected to the transformer are ignored. In the simulation of voltage stresses, the coil is considered at the beginning of the coil, which can significantly model the bushing effect on the behavior of the transformer. In the layering of the internal components of the transformer, the coils of the transformer are in the form of three separate coils on the common core. For each coil, the high voltage coil in the upper layer and the low voltage with the higher current are wrapped below it. The transformer core is commonly used in multi-layer. Core edges are rounded as much as possible. This is done to avoid the accumulation of loads at a single point and a uniform flow of flux [13]. In this paper, instead of creating a model with multi-layer core and rounded edges in simulation geometry. The effect of the conventional geometry of the

transformer core in the simulation magnet module is applied with a coefficient of 20%. The position and configuration of transformer components are as shown in Fig. 1.

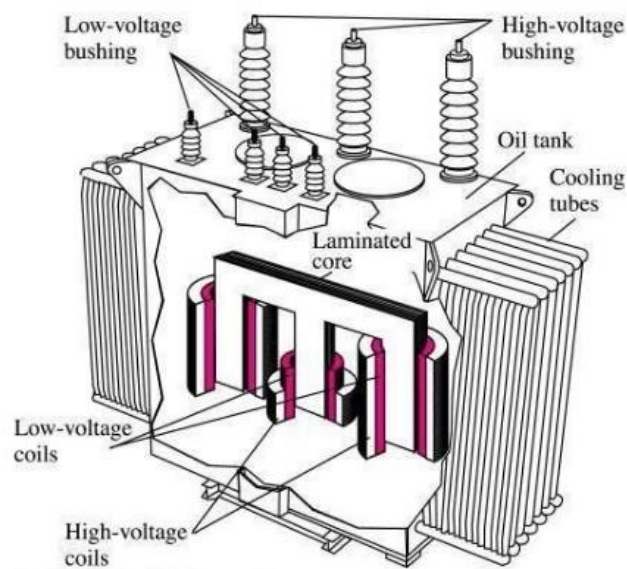


Fig 1. Transformer parts.

By entering the above values in the Comsol simulation environment, the 3D image of the model in the software is in Fig. 2.

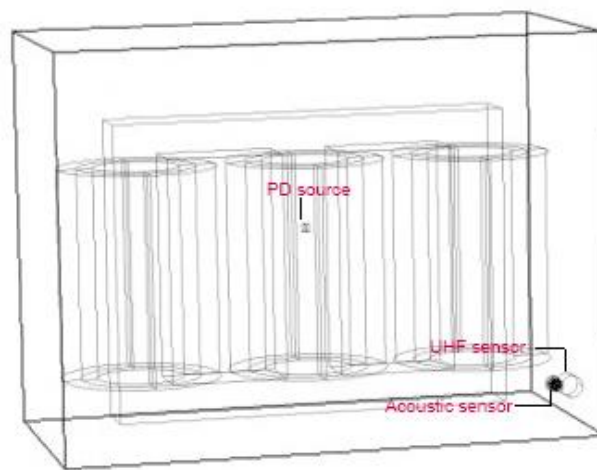


Fig. 2. Simulation geometry.

Three relevant geometries on the Comsol should be created. The data used to create the geometry of transformers, sensors (acoustic and UHF), and the source of partial discharge are as follows. Transformer, Sensors, and PD's cavities are based on Table 1.

Elements used in the experiment are as follows: 1MVA three-phase transformer manufactured by Iran Transfo Co., the Acoustic sensor (R30α) and UHF sensor (standard UHF

drain valve DN80). Data used in the simulation is entirely based on the actual values of these elements. The geometry of the sensors implemented in Comsol shown in Figure 3.

**Table 1. Geometry dimensions**

Quantity	Values (mm)
Transformer's tank Dimensions	1492*730*1108*112
Coil Dimensions	580*220
Transformer's core Dimensions	1080*150*820
Acoustic sensor shell	8.7*28.8*3
cylindrical cavity Dimensions	9*20
Acoustic sensor diaphragm, piezoelectric, holder height	0.3, 9.4 ,14.2
Acoustic sensor connector space	4.9
Uhf sensor Dimensions	83*39
Uhf sensor receiver Dimensions	24*42

After applying these dimensions, the simulation of the final geometry is shown in Fig. 4.

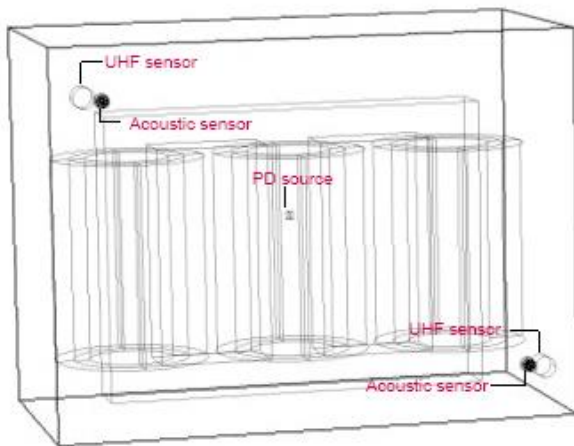


**Fig. 4. Final geometry on COMSOL Multiphysics 5.2a.**

## 2.2 Model

### 2.2.1 Model Components Material Properties

Comsol allows you to apply the material used in making various components of the model. This will increase the quality of simulation by interacting material properties in the process and simulation calculations.

**Tank:** The transformer tank is made of sheet metal with a thickness of 11.2 mm. This characteristic (thickness) has been applied in geometry and Properties of the sheet used are identical in the material library (Iron), and only the reflection

index is considered non-losses, which is reasonable considering the size of the sheets.

**Transformer oil:** In Iran Transfo's 630 kVA Transformer, has been used transformer oil of Zangan Company. In this study transformer, 296 Nero Zangan oil was used. This oil filled the entire space of the transformer tank and the space between the insulating layers of the windings. This oil is based on IEC 60296, which is why it is similar to the specifications of the transformer oil in Comsol the Materials Library. Only changes made by Table.2 apply. (data from company catalog)

**Table 2. Revised Transformer Oil Specification**

Density at 20°C	0.85 kg/dm <sup>3</sup>
Sludge	1%
Breakdown voltage	52/76 kV

**Core:** The core of the transformer is modelled based on non-leakage. In practice, the losses of the transformer are not very effective in measuring the discharge rate.

**Coils, UHF receiver:** The coils are selected in primary and secondary groups of different sizes, but the specifications of the copper are the same. Alloys in practice when converted to a coil in the form of contamination, bending, and surface scratches, change their specification, which changes the overall magnetic profile. These variations are negligible. This value is often less prevalent in similar studies — 1 and close to zero. However, to improve the accuracy and quality of the simulation in this study, the variation in all specifications of this material is considered to be 1%. It is the same for the UHF antenna.

**Air:** Around the transformer's space and the hole in which a partial discharge occurs is modeled with air. This material comes from the Comsol Library without changing it.

**Piezoelectric ceramics:** This material is available in the software library and will be introduced further[14, 15].

**Sensor shell:** The shell of the sensors is steel. This material is available in the Comsol Materials Library without modification.

### 2.2.2 Modules

To complete the simulation, use the Comsol's modules to apply the desired processes. To create different parts of the

model, use the ACOUSTIC, AC/DC, and RADIO FREQUENCY modules. In the following, setting up the physics of the structure of the above modules to build the final model.

#### 2.2.2.1 Magnetic and Electrical circuit

For the magnetic analysis of the transformer during the central phase of the pregnancy, it will apply the values of the transformer model. Because of the importance of the core effect and the possibility of magnetic core tracking, model the structure of the core effect model with the use of a Transformer Equivalent Circuit[16]. To apply the equivalent circuit for a three-phase transformer, use a single-phase equivalent circuit[17, 18]. Transformer equivalent circuit is simplified according to Fig. 3. Which is applied for each phase independently? Circuit values from the manufacturer's laboratory have been queried. Other specifications based on Table.3 is entered in physics. The basic equations for the magnetic transformer simulation are shown in Table 3. Considering the magnetic properties of the transformer is only due to the closest simulation to the actual study sample. That is why there is no need to apply the equations added to the basic equations.

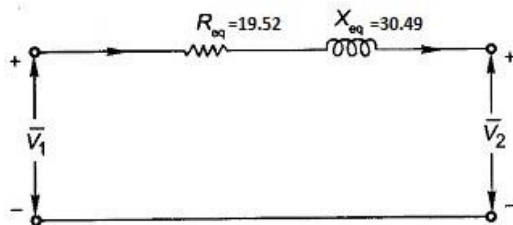


Fig. 5. Transformer Equivalent Circuit

Table.3. Parameters of magnetic and electrical physics of the simulation model

Parameter	Value
Vector Group	Dyn5
Frequency	50 Hz
Primary voltage	20 kV
Secondary voltage	0.4 kV
turns of the primary coil	1.9e5
turns of the Secondary coil	1.4e4
$\Delta V$	1.4%
Voltage insulation for the primary winding	50 kV
Voltage insulation for Secondary winding	3 kV

After applying the values and equations above in the simulation platform, the 3D output from the transformer's magnetic stimulation (normal operating mode) will be in

Fig. 6.1. Moreover, Figure 6.2. Shows the normal operation mode of the transformer for Energize the transformer's central coil.

Tale.4. the basic equation for magnetic and electrical physics of the simulation model

$\nabla \times H = J$ $B = \nabla \times A$ $J = \sigma E$	General equation assuming
$n \times A = 0$	General equation insulation
$D = \epsilon_0 \epsilon_r E$	Electric field
$B = \mu_0 \mu_r H$	Magnetic field

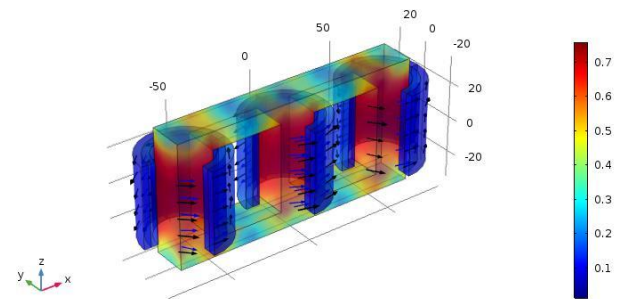


Fig. 6.a. Normal operating mode (3 phase).

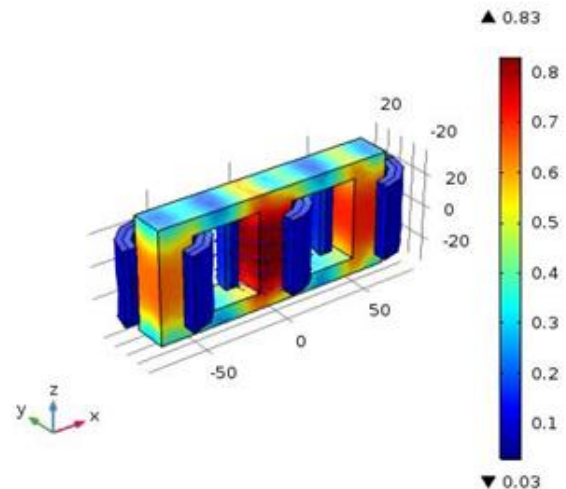


Fig. 6.b. Normal operating mode (1 phase).

#### 2.2.2.2 Acoustic

The next step is to model the acoustic wave propagation in transformers using Comsol's acoustic module. The Comsol's Acoustic Module is a collection of physics interfaces that can cover all-acoustic simulations in fluids and solids. Acoustic modeling typically consists of three main components: Sound source, emission environment, and boundary properties of the emission environment, the

receiver [19]. Accordingly, this part of the simulation is completed in three steps. The acoustic source in this simulation is a cavity with active PD in it. The acoustic wave propagation environment includes transformer oil, coils, and transformer core. The acoustic signal receiver is a piezoelectric sensor[20]. Capacity and partial discharge power are performed by changing the cavity size. The main problem for acoustic emission is the complex nature of acoustic wave propagation. Although the partial discharge source is small enough to be seen as a point source of acoustic, and due to the nature of the wave propagation, spatial sources produce spherical wave angles[21, 22]. To recognize the authenticity of the acoustic-based partial discharge signal, two parameters of the wavelength and Rise Time of First Oscillation increase are considered[23]. As a result, to generate an acoustic partial discharge signal, it is enough to produce these two parameters artificially. Simulations based on numerical modeling of each shape of the partial discharge wave that the sensor receives represents the path that the signal has passed[24]. However, the advantage of simulating geometry with Comsol such as a commissure is that when in this work simulate the discharge source, by placing the sensor at the desired location, can have the signal by applying the effect of the path just like a real measurement in the transformer. To calibrate the simulations in this study is a partial discharge of 150 pC is considered, with a frequency of about 100 kHz[25]. As a result, instead of modeling a static PD source, create a dynamic PD source that is used throughout the encoder, and one pC, 50 pC, 150 pC tree points are used as the main points of the function to calibrate the source changes. The governing equations of acoustic simulation based on Table 4 arrived. To maintain simulation accuracy, the frequency generator of the emission of both acoustic and

electromagnetic signals must be the same. In this paper, the Gaussian pulse is selected as the drive of both simulations. This will create the required similarity. The activity sample of this Gaussian pulse for acoustic signal propagation is Fig. 6. Equation (1) will be the equation for acoustic wave propagation Generated by Partial Discharges:

$$y_i(t) = \frac{A}{1+ae^{-b(t-\tau_i)}} e^{-\frac{(t-\tau_{2i})}{\gamma}} \times A_{\cos i} \cos(2\pi f_i(t - \tau_{3i})) \quad (1)$$

where, an amplitude of the sigmoid function (V),  $a$  scale coefficient of the sigmoid function,  $b$  shape coefficient of the sigmoid function,  $\tau_1, \tau_2, \tau_3$  localization coefficients (s),  $\gamma$  — shape coefficient of the exponential function,  $f$  frequency of the cosines function (Hz),  $A_{\cos}$  amplitude of the cosine function,  $t$  time (s)[26]. Equation (1) will be the base equation for acoustic wave propagation in one dimension:

$$\nabla^2 p - \frac{1}{c^2} \frac{\delta^2 p}{\delta t^2} = 0 \quad (2)$$

where,  $\nabla^2$  is the Laplace operator,  $p$  is sound pressure,  $c$  is the speed of sound in m/s, and  $t$  is a time in second.

$$c^2 = \frac{\delta p}{\delta \rho} \quad (3)$$

where,  $p$  is the pressure and  $\rho$  is the density and for Sound pressure level used for equation (2).

$$L_p = \ln\left(\frac{p}{p_0}\right) \quad (4)$$

where,  $p$  is sound pressure of point,  $p_0$  is reference sound pressure [24, 27-31].

**Table 5. Equations governing the acoustic simulation**

$\nabla \cdot \left( -\frac{1}{\rho_c} (\nabla P_t - q_d) \right) - \frac{K_{eq}^2 P_t}{\rho_c} = Q_m$ $P_t = P + P_b$ $K_{eq}^2 = \left( \frac{\omega}{C_c} \right)^2$	General equation assuming
$-n \cdot \left( -\frac{1}{\rho_c} (\nabla P_t - q_d) \right) = 0$	Boundary equation assuming
$-n \cdot \left( -\frac{1}{\rho_c} (\nabla P_t - q_d) \right) + \left( iK_{eq} + \frac{1}{r_{rf}} \right) \frac{P^2}{\rho_c} - \frac{r_{rf} \Delta_T P^2}{2\rho_c (1 + iK_{eq} r_{rf})} = Q_i$ $r_{rf} =  (x - r_0) $	Radiation equation assuming
$\nabla \cdot \left( -\frac{1}{\rho_c} (\nabla P_t - q_d) \right) - \frac{K_{eq}^2 P_t}{\rho_c} = \frac{4\pi}{\rho_c} S \delta(x - x_0)$ $S = e^{i\phi} \frac{i\omega \rho_c Q_s}{4\pi}$	Source equation assuming



Simple of Comsol acoustic module's configuration is shown as in Fig 7.

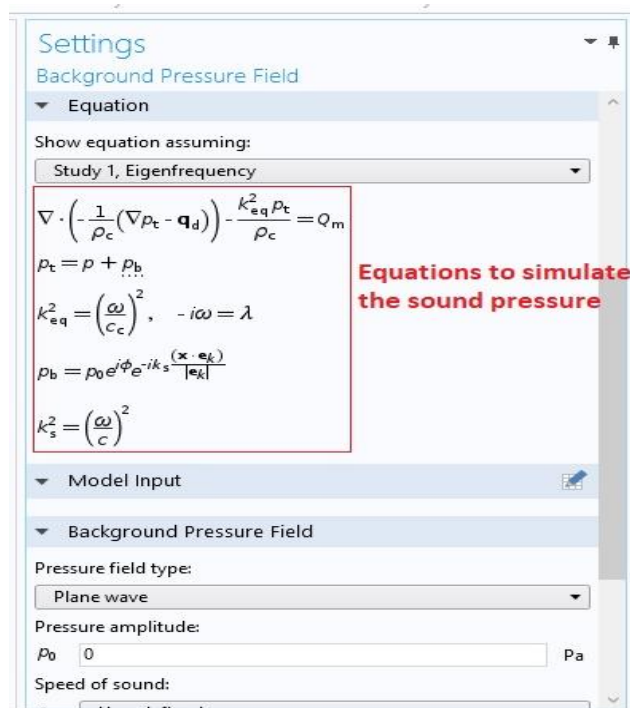


Fig. 7. Sample Configuration Acoustic Module on COMSOL 5.2a.

The 3D output of the acoustic wave pressure emission simulation at 200 kHz is shown in Fig. 8

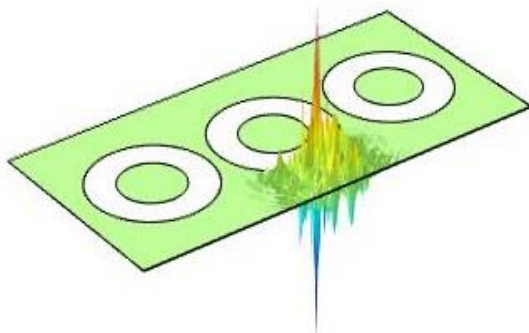


Fig. 8.a. Gaussian pulse for acoustic signal.

For modeling, the acoustic sensors, one of the best ways to simulate is based on the actual sample shown in Fig. 9. The main components of the acoustic sensor are Piezo Ceramic, Electrode, and Diaphragm, which is modeled according to the values of Table 5 as Fig. 9.

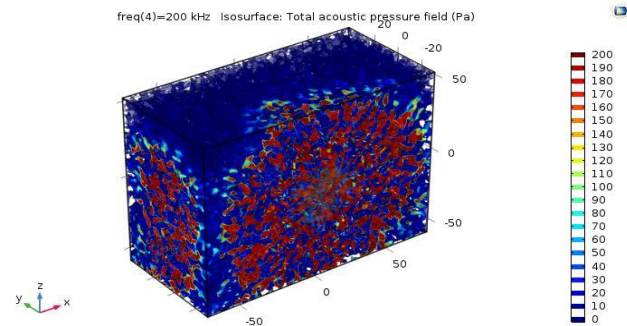


Fig. 8.b. Acoustic pressure at 200 KHz.

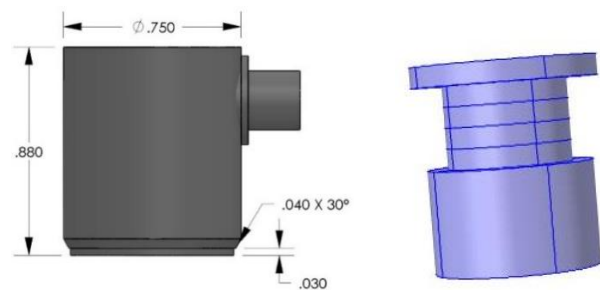


Fig. 9. piezoelectric sensor.

The acoustic sensor output is in Fig. 10.

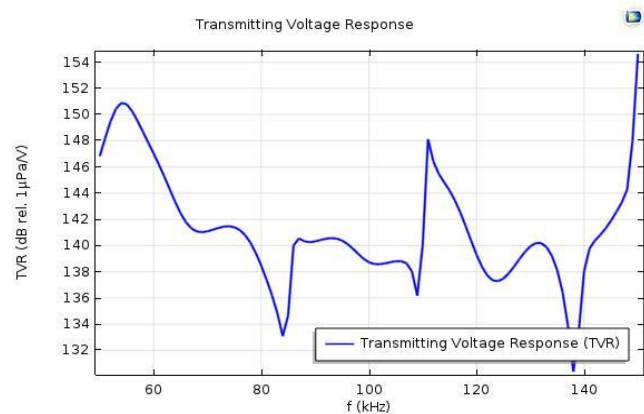


Fig. 10.acoustic sensor voltage response.

### 2.2.2.3 Radio Frequency (RF)

The (UHF) Detection Method is one of the methods for online PD Detection in Power Transformer [32]. One of the main advantages of this type of detection allows continuous online monitoring signals for partial discharge, and it can be determined the type of the partial discharge's source used UHF signal [33, 34]. These two of essential advantages of UHF detection method are commonly used in comparison with the conventional detection method. Although productivity and research on the use of UHF detection in the last decade have intensified. However, in this case, the study is a step forward. The results of an experimental

measurement show that the forehead of the discharge wave is less than 50 ps and the frequency spectrum has components of about 8 GHz. Various evacuation pulses have different timing and frequency spectra. As a result, Can be used by [35] According to real experiments and by matching the measurements done ,can simulate a partial discharge signal with high quality for the model transformer and with a low emission error. As a result, some master signal's parameters have been created with the help of [35]. The reason for this choice is to keep the source of the partial discharge equal. The result can create acceptable similarity with its acoustic simulation. Differences in simulations are related to the high-level measurements of the components due to the diffusion of the signal emission location. With changes simulated used [33, 36]as far as possible, it is set to zero. In this paper, instead of using a numerical model for electromagnetic wave propagation to simulate wave frequency behavior at high frequency. In this study, the properties of antennas are used to generate a high-frequency wave. It seems that the occurrence of partial discharge inside a small oily cavity (discharge cavity) is very similar to that of Antenna, and the greater the unstable potential difference in the both cavity's side increases this similarity. As a result, partial discharge at high frequency and location on the coil is modeled as a bipolar antenna[34, 37, 38]. And as an antenna drive, use the Gaussian pulse. As the base equation of wave simulation is considered in equation 5:

$$\nabla \times \mu_r^{-1}(\nabla \times E) - K_0^2 \left( \epsilon_r - \frac{j\sigma}{\omega\epsilon_0} \right) E = 0 \quad (5)$$

As it is known, the variables of the above equation are identical with the variables of the equations in the previous section. For this reason, it can generate homogeneous simulation. To calibrate the electromagnetic emission's

simulation like the acoustic emission simulation, used the IEEE standard draft has.

Assuming Equations to simulate shown in Table 3.A number of values for modeling the emission of electromagnetic waves is shown in Table 3. So the remaining amounts from the material's library have been directly entered into the simulation[39-42].

The UHF antenna is calculated from equation 6,7:

$$E_\theta = j\eta \frac{I_0 e^{-jkr}}{2\pi r} \left[ \frac{\cos\left(\frac{\pi}{2} \cos\theta\right)}{\sin\phi} \right] \quad (6)$$

$$H_\theta = j \frac{I_0 e^{-jkr}}{2\pi r} \left[ \frac{\cos\left(\frac{\pi}{2} \cos\theta\right)}{\sin\phi} \right] \quad (7)$$

$r, \theta, \phi$  respectively the growth rate, angle measurement of the axis and angle measured counterclockwise of the axis and other parameters are like previous equations [43, 44].final simulated antenna as shown in Fig.11.

The final output of the sensor (Antenna) is shown in Figure 12.

#### 2.2.2.4. Meshing

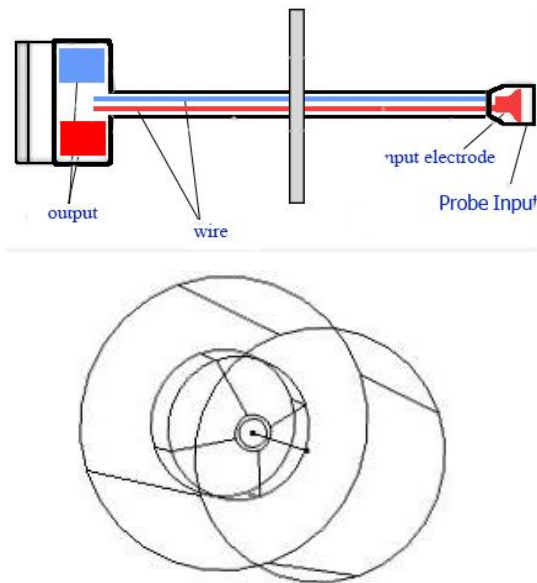
To solve the equation by the finite element method, most meshed the simulation geometry. The smaller mesh size gives higher accuracy in calculations. However, to do calculations with small mesh, need a stronger workstation for computing. Which requires a stronger processor and more volume of RAM. The calculations with large mesh are fast and do not require a robust workstation. However, the accuracy of these calculations is poor. Therefore, must be appropriate mesh size to establish a fit between accuracy and speed in the calculation [48, 49].

**Table 6. RF equation assuming**

$n \times E = 0$	Conductor equation assuming
$\sqrt{\frac{\mu_0 \mu_r}{\epsilon_0 \epsilon_r - j\sigma/\omega}} n \times H + E - (n \cdot E)n = (n \cdot E_s)n - E_s$	Impedance equation assuming
$f_{c(m,n,p)} = \frac{c_0}{2\sqrt{\epsilon_r}} \sqrt{\left(\frac{m}{height}\right)^2 + \left(\frac{n}{width}\right)^2 + \left(\frac{p}{depth}\right)^2}$	Resonance Frequency equation assuming
$Z = \frac{V_1}{I_1}$	Source equation assuming
$n \times (\nabla \times E) - jkn \times (E - n) = 0$	Scattering equation assuming
$S = \frac{\int_{\delta\Omega} E \cdot E_2}{\int_{\delta\Omega} E_2 \cdot E_2}$	Channel equation assuming

**Table 7. RF cavity data**

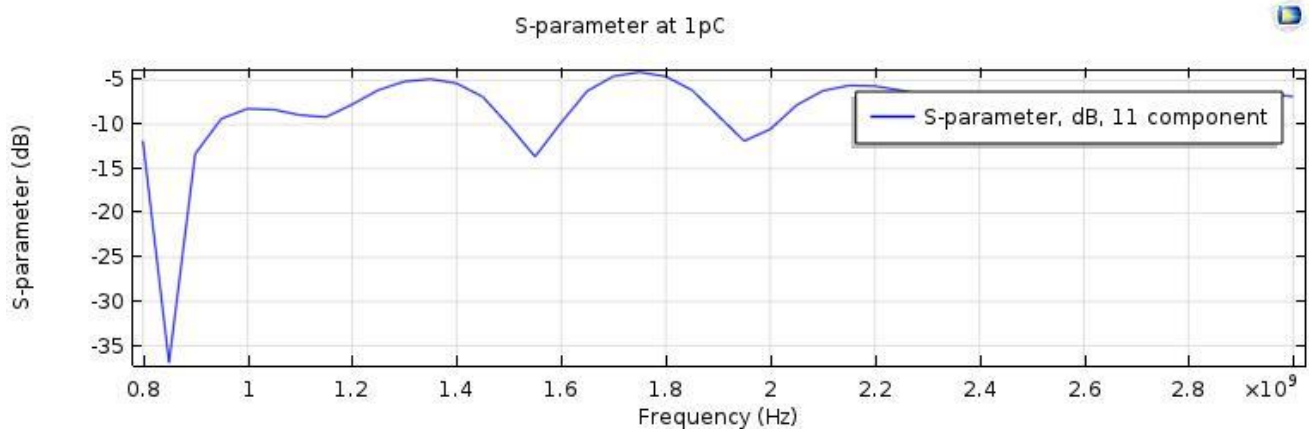
$\epsilon_r$	2.16
UHF wave generator gap	0.4 mm
Frequency range	850 MHz-3000 MHz
Step frequency	10 MHz
Impedance	50 $\Omega$

**Fig. 11. UHF antenna.**

The best way to meshing geometry on COMSOL used COMSOL's auto meshing. To solving this problem, the second-order LaGrange is commonly used. This is a rule for

averaging in determining the size of the element. This rule is based on wavelength work[45]. However, this simulation uses a wide range of wavelengths (40 kHz-1.5GHz); for this reason, applying this rule will be a complication. As a result, define several conditions for applying wavelength. The maximum wavelength used in this simulation is 7500m (10 kHz), and the lowest applied 200 mm(at 1.5 GHz). To ensure the proper mesh size section, there must be two-second order elements per each half period. So the problem is not meshing at high frequency. The problem is the proper mesh at the acoustic frequency. Therefore, the first condition is the mesh dependence of the acoustic — model's frequency. Components of different sizes are used in the model geometry. So the smallest mesh element size is smaller than the smallest model components element size [46]. This is the second condition imposed on the mesh size. The remaining decisions are taken automatically by COMSOL.

As it is known, the variables of the above equation are identical with the variables of the equations in the previous section. Therefore, it can generate a homogeneous simulation. To complete the modeling of PD cavity's wave propagation used the Comsol's RF module to configure the emission of electromagnetic waves. The advantage of this is relative to the manual equation; the emission of acoustic and electromagnetic waves has an equal accuracy [39, 40]. As previous step, all parameters are called from the material library. By applying automatic Comsol's meshing and using the PC (personal computer) with AMD Ryzen 7 1700X Processor, 64 GB of DDR4 memory and 256 SSD hard. The duration of the simulation with this pc was 1151 minutes (19h 11m 21s)., the result of acoustic and electromagnetic wave propagation simulation of partial discharge activity shown in Figure 13.

**Fig. 12.UHF sensor response.**



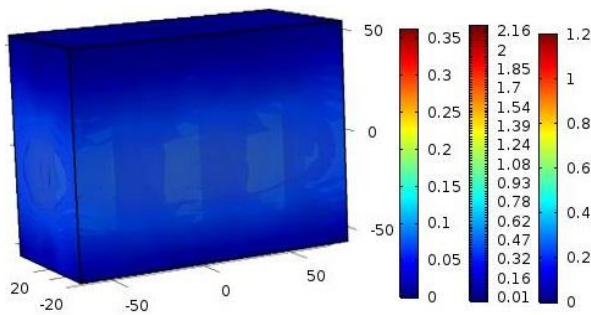


Fig. 13. Sample Configuration Acoustic Module on COMSOL 5.2a.

### 3. MATLAB INTERFACE AND DATABASE CREATION

First, on Comsol, create a link with MATLAB. Next, create a database on MATLAB with the following fields: PD charge, PD source location, sensor response (separate matrix for acoustic and UHF sensor) [47]. PD charge is given as an input to the PD source for generating the acoustic and UHF waves. To build this database, most move the PD source into the simulated transformer with specific steps. To do this, consider the transformer as an empty tank, which is laminated with xy plat. Also, repeated until hz (height of Z plane) with the desired step. The problem space is now transformed from 2D into 3D. In the next step, consider the page as parallel to the x-axis, which is perpendicular to the y-axis and is repeated with the same Z-step. By moving the PD source on these lines with the same z step, move the source into finite difference squares that can be the best interface between MATLAB and Comsol. Create the database manually requires much time. To solve this problem, we use the script code in MATLAB. The inputs of this code are the length, width, and height of the transformer tank as the 3D source space movement. The response patterns of the sensors are generated for 0 pC (no PD) to 400 pC charge at 0.1 steps. After completing the movement of PD source in the simulation space, increase the charge of PD source adds 0.1 up. Therefore, Comsol's input and output data are making the pattern database.

One of the most important challenges is to recognize the pattern of text or image conversion into numeric strings, so can do math or matrix operations. However, in this work, both imported data from the Comsol software and oscilloscope connected to the sensors are imported numerical strings into the MATLAB. For this reason, one of the most important challenges in pattern recognition is missing in this study. Moreover, just enough, set the equal sample rate for Comsol and oscilloscope output. The sample rate was 0.1 at this rate. It now can create weighted data strings by doing mines operations on the numerical strings generated by the software and numerical strings generated by sensors. The result of each of these calculations, which is closer to the zero number, is the two strings most closely resembling each other. To reduce the decimal number, used

modulus operation in this calculation. However, that, given the numerical range of the graphs, does not significantly affect the accuracy and quality of the study. In the graphic interface, the nnz command is used to specify non-zero elements, and the numel command is the total number of elements, and the difference between these two elements is zero, and in fact, the weight of the string is determined. Also, the command loop, according to the flowchart, chooses a final string.

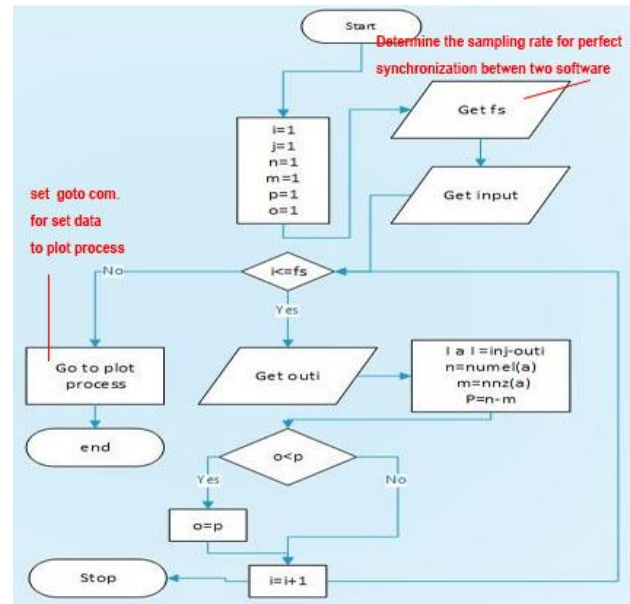


Fig 14. Pattern recognition algorithm.

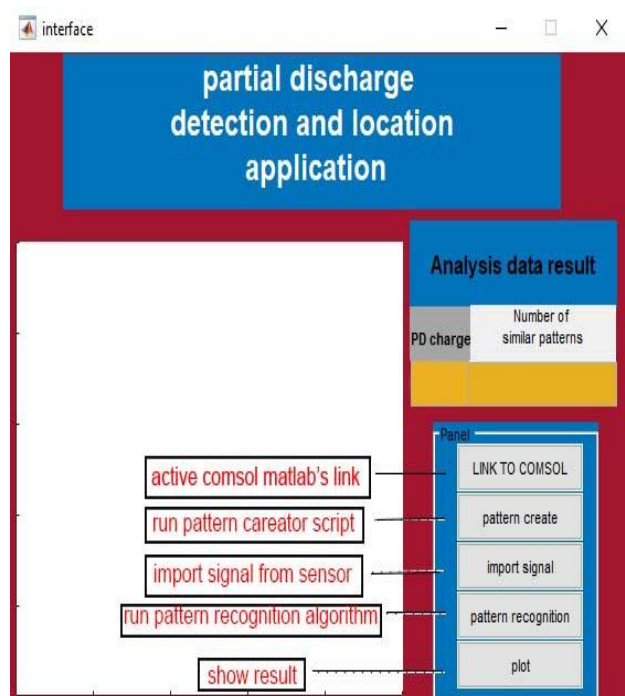


Fig 15. Matlab's interface.

The simplicity of the operation performed in this diagnosis has a significant effect on the speed of the work. Which ultimately leads to the running of this software on most portable computers.

Also, we need to enter simulating numeric strings to the software database. This technique is similar to the interlocking algorithm used in vision machines. In practice, by eliminating single-by-one cases, the answer is reached. Pattern recognition algorithm for the searching database to find the most similar data to the oscilloscope signal output is shown in Figure 14. also, Matlab's interface shown in Figure 15.



Fig. 16. PD source (electrode) & PD calibrator (set at 10 pC).

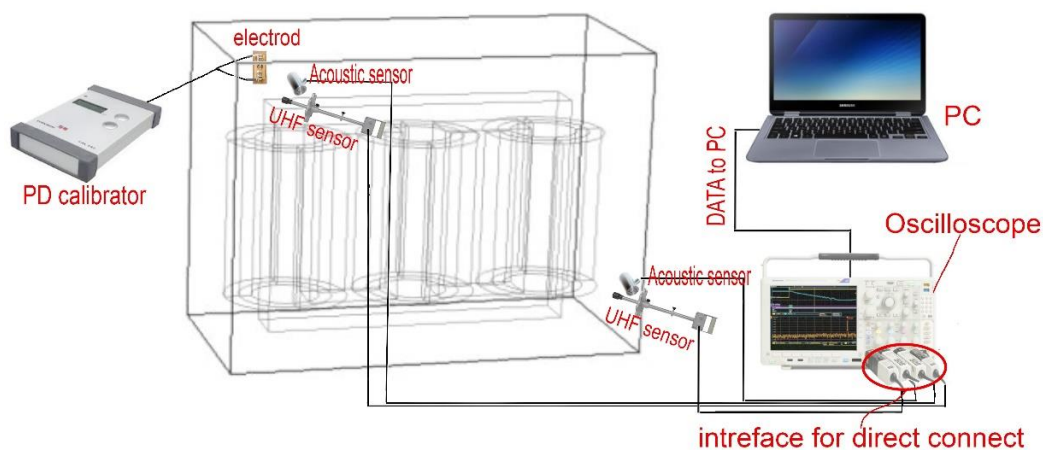


Fig. 17. Test setup.



Fig. 18. PD source (electrode) and sensor location.

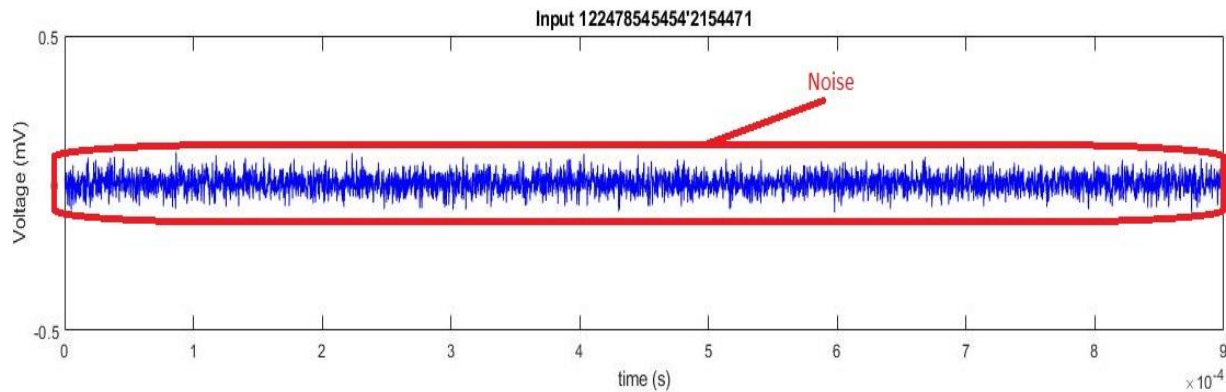


Fig. 19. Signal received from the UHF sensor (PD source is not activated).

The test setup is shown in Figure 17.

#### 4. EXPERIMENTAL TEST

One of the most critical parts of any new idea is tested with a sample of experimental Verification. There are two ways to do this work in practice. Comparing the results of simulated samples with results of experimental measurement or inquiring a new method for solving a real problem that already knows the answer. The second method is used in this work. Therefore, the final comparison for verifying the method presented in this article will be between the result of the paper method and the predetermined response. The deviation of these responses are closer to zero; the new method is more accuracy and efficiency. To improve test accuracy must PD source signal is accurate; for this purpose, A PD calibrator connected to the electrode as shown in Fig.16 has been used as the PD source on the transformer. By connecting the electrode to the calibrator, can generate sparkers as much of charge size given to the calibrator with a standard distance of 1 millimeter can be produced.

To remove noise from the main signal, first, the analog noise signal converted into a digital noise signal. The digital signal noise sampling rate must be the same as the original digital signal. The sampling rate in this research was 150 kHz acoustic signal and 850 MHz for UHFsignal[48].

The Signal showed in Fig. 19 as a Published acoustic signal in typical operating mode transformer is recorded. This signal combined noise and so small PD signal. By removing this signal from the primary signal when PD activity can be recorded in an evacuation signal was free of noise[49].

For create online application can be connected an oscilloscope to the PC forgive the sensor's data and transmit it to the application. However, in this study Data was transferred to the computer via USB drive because only four data string has been received from the oscilloscope. The oscilloscope output is shown in Fig. 20.

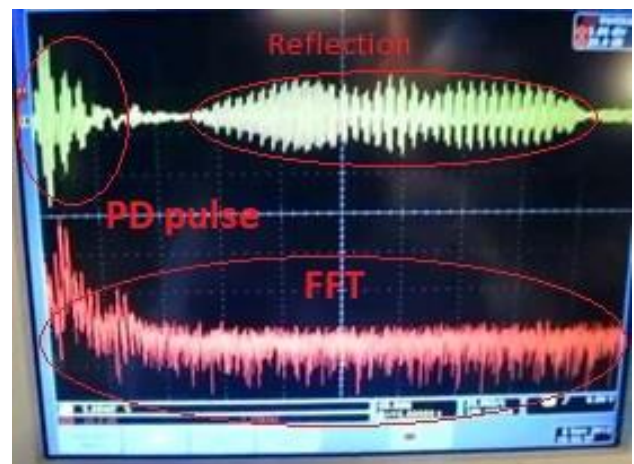


Fig 20. Acoustic signal (frequency domain & time domain)

After entering the analog data into MATLAB, the digital output form will be as Figure 21.

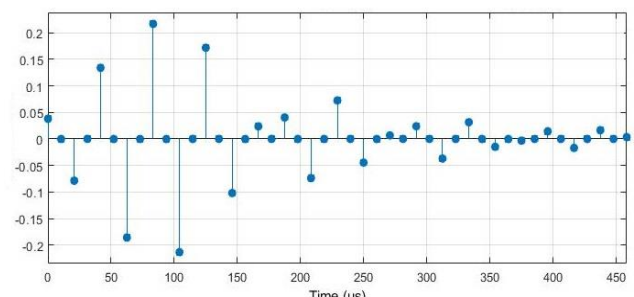


Fig 21. Digital signal.

To get a better result, choose the original signal range from the oscilloscope when taking the data. By entering the signals received from the sensors of group 1 (group number shown in Fig. 9), the software designed in MATLAB will display the output of the software as Fig. 22.



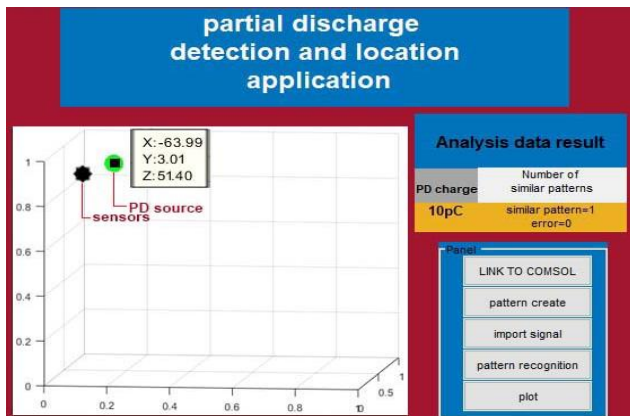


Fig 22. Software output

As indicated in the output form of the software, the location of the PD source and the discharge size are accurately detected. Once again repeat an experiment to sensor group 2. The location of the sensors in group 2 is inappropriate for detecting PD source. Makes it difficult to detect a PD source. That is why this test could be a good test

for the accuracy of this presented method. For this case, the result is, as shown in Figure 23.

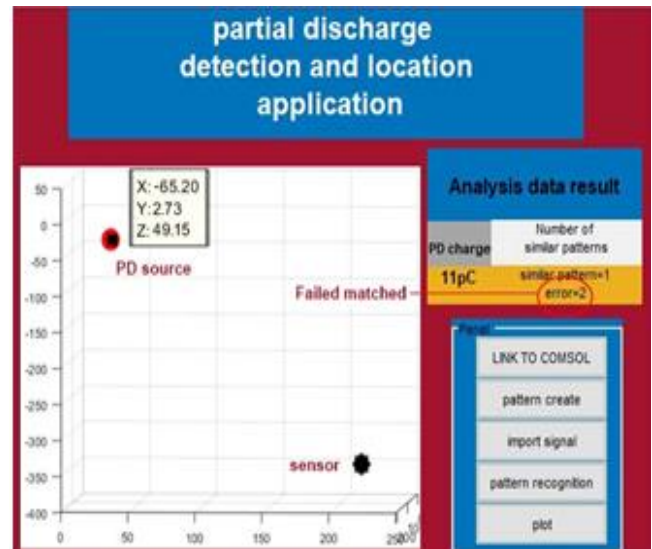


Fig 23. Software next output.

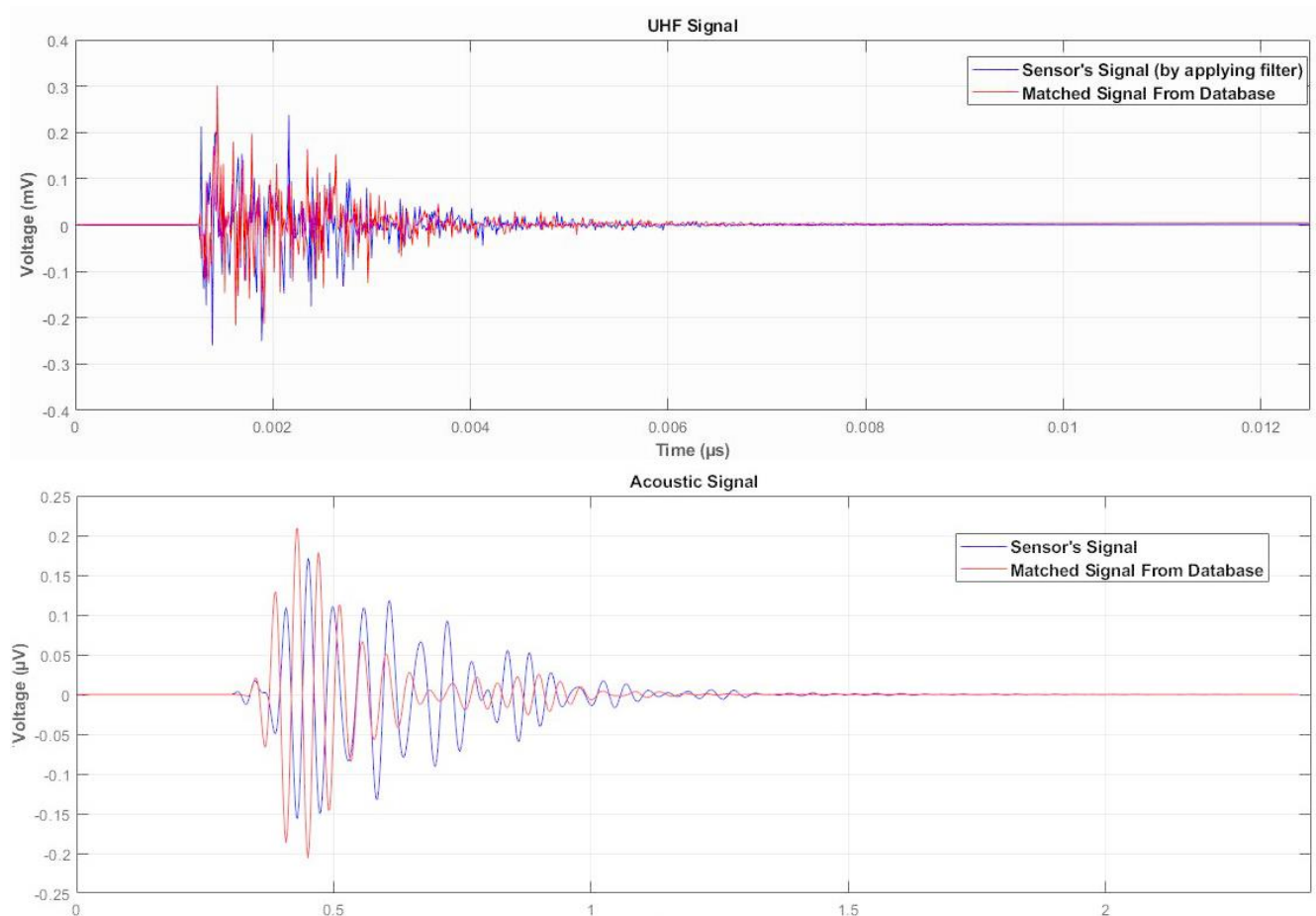


Fig 24. Matched signal (Sensors Group 2).

In this case, with two errors, the closest response to the input signal is found by the software. The result of matching the received signal and the database patterns that the software output is based on is shown in Figure 16. On the signal is shown in figure 14 with the two filters, the Noise removed and normalization filter is applied. The received UHF sensor's signal when the partial discharge is not activated, removed from the original signal as the ambient noise. The signal sample is shown in Fig. 24. As shown in the figure. Adaptation of the original signal and the simulation is very high. In this case, for example, to be precise is 95.713%. The amount of similarity, as well as the accuracy of the simulation, reveals.

## 5. RESULTS

To maintain the accuracy of signal analysis, for both cases, the same filter is applied. The received data from the sensors is recorded by the oscilloscope alone. Due to minimizing the comparison is shown in Table 4. According to Table 4, the method presented in this paper with  $\pm 2$ cm measurement accuracy, considering the size of the transformer's tank and the sensor's position has the right accuracy. In sensor group 2, the most error is related to the axis X, and the most significant variation of distance is related to this axis. Due to the low PD charge (10 pC), the response deviation was as low as one pC. The presented results are all based on the analysis algorithm is shown in table8. The accuracy of calculations based on full convergence results in MATLAB is.

**Table 8. Comparing the test mode with the original answer**

Case	X (cm)	Y (cm)	Z (cm)	Charge (pC)
1	-63.99	3.01	51.49	10
2	-65.20	2.73	49.15	11
Main	-63	3	52	10

## 6. CONCLUSION

In this work, presented a new method for detection and location of PD using Patterns database created on MATLAB by COMSOL output data and only one of real acoustic and UHF sensor as input data (sensor signal) to an application designed in MATLAB. Finally, the validity of this method is determined by comparing the results of the practical test and the method results. Conclusion as follows:

- Practical test performed to validate this method show as well as the ability of the presented method to detection and location of partial discharge in power transformers. The low deviation of the verification test result from the primary response confirms the validity of this method ( $\pm 1\%$ ).

- Using only one sensor in this method, that makes an inexpensive and secure method. Database creation method in this paper can be used to create a comprehensive database

from all produced power transformers. So by using the presented PD detection method, create the software for detection and location of partial discharge in power transformer.

- As a byproduct, according to the performance of database creation and validation test can be said is accurate sensor simulation. Therefore, the method of simulating sensors in this paper can be presented as a new method. Also, with the possibility of converting the Comsol's simulated model to the MATLAB's m-file, the models can be easily inserted into MATLAB.

- The cost of this method vs. other methods is meager.
- The accuracy of this method and other methods of identification of PD is approximately equal.

## REFERENCES

- [1] P. RezaeiBaravati, et al, 2014"Transformer winding modeling based on multi-conductor transmission line model for partial discharge study" Journal of Electrical Engineering and Technology, 9 (1), pp. 154-161.
- [2] P. RezaeiBaravati, et al, 2015 "Partial discharge localization based on detailed models of transformer and wavelet transform techniques" Journal of Electrical Engineering and Technology, 10 (3), pp. 1093-1101.
- [3] SMH Hosseini, SM Enjavimadar, M Vakilian, 2015 " Using the finite element method to calculate parameters for a detailed model of transformer winding for partial discharge research" Turkish Journal of Electrical Engineering & Computer Sciences 23 (3), 709-718.
- [4] Cattareeya S., Pongsakorn T., Sayan R., and Thanapong S., Partial Discharge Detection in High Voltage Equipment Using High Frequency Current Transducer, GMSARN International Journal 7 (2013) 53 - 58.
- [5] Mishra, D.K., et al., Self-organizing feature map based unsupervised technique for detection of partial discharge sources inside electrical substations. Measurement, 2019. 147: p. 106818.
- [6] Coenen, S., et al., Sensitivity of UHF PD measurements in power transformers. IEEE Transactions on Dielectrics and Electrical Insulation, 2008. 15(6): p. 1553-1558.
- [7] De Kock, N., B. Coric, and R. Pietsch, UHF PD detection in gas-insulated switchgear-suitability and sensitivity of the UHF method in comparison with the IEC 270 method. IEEE Electrical Insulation Magazine, 1996. 12(6): p. 20-26.
- [8] Raja, K., F. Devaux, and S. Lelaidier, Recognition of discharge sources using UHF PD signatures. IEEE Electrical Insulation Magazine, 2002. 18(5): p. 8-14.
- [9] Hoshino, T., S. Maruyama, and T. Sakakibara, Simulation of propagating electromagnetic wave due to partial discharge in GIS using FDTD. IEEE Transactions on Power Delivery 2009. 24(1): p. 153-159.
- [10] Rutgers, W. and Y. Fu. UHF PD-detection in a power transformer. in 10th International Symposium on High Voltage Engineering. 1997.
- [11] Nadja, J., On simulation of surface discharges at variable voltage frequency. 2007, Stockholm, Sweden: The Royal Institute of Technology.
- [12] [12] Tavakoli, B., Hosseini, S. M. H, Comparison the PD



- Current and PD Voltage for Two Cubical and Cylindrical Cavity in Solid Insulation Resin Epoxid, GMSARN International Journal 14 (2020) 97 - 103.
- [13] Leite, J.V., et al., Finite element three-phase transformer modeling taking into account a vector hysteresis model. IEEE Transactions on Magnetics, 2009. 45(3): p. 1716-1719.
- [14] Jiang, Y., et al., Preparation and characterization of  $y\text{BiGaO}/\text{sub } 3/(1-xy) \text{ BiScOs}/\text{sub } 3-x/\text{PbTiO}/\text{sub } 3$ /piezoelectric ceramics. IEEE transactions on ultrasonics, ferroelectrics, frequency control 2007. 54(12).
- [15] Seo, I.-T., et al., Microstructure and piezoelectric properties of (Na 0.5 K 0.5) NbO 3 lead-free piezoelectric ceramics with V 2 O 5 addition. IEEE transactions on ultrasonics, ferroelectrics, frequency control 2009. 56(11): p. 2337-2342.
- [16] Javadi, S., B. Vahidi, and S. Hosseinian. Three phase transformer modeling with consideration the core effect. in Electrical Machines and Systems, 2008. ICEMS 2008. International Conference on. 2008. IEEE.
- [17] Prochazka, R., J. Hlavacek, and K. Draxler, Magnetic circuit of a high-voltage transformer up to 10 kHz. IEEE Transactions on Magnetics, 2015. 51(1): p. 1-4.
- [18] Noah, M., et al., Magnetic Design and Experimental Evaluation of a Commercially available Single Integrated Transformer in Three-phase LLC converter. IEEE Transactions on Industry Applications, 2018.
- [19] Mazlomii, S. M. and Hosseini. S. M. H., Diagnosing and Online Partial Discharge Location with Using Coupling Capacitor in Induction Motors, GMSARN International Journal 17 (2023) 319-328.
- [20] Platt, S.R., et al., The use of piezoelectric ceramics for electric power generation within orthopedic implants. IEEE/ASME Transactions on Mechatronics, 2005. 10(4): p. 455-461.
- [21] Palmeri, M.L., et al., Guidelines for finite-element modeling of acoustic radiation force-induced shear wave propagation in tissue-mimicking media. IEEE Trans Ultrason Ferroelectr Freq Control, 2017. 64: p. 78-92.
- [22] Zhang, B., et al., Modeling and analysis of lateral propagation of surface acoustic waves including coupling between different waves. IEEE transactions on ultrasonics, ferroelectrics, frequency control, 2017. 64(9): p. 1354-1360.
- [23] Traore, O.I., et al., Impact of the Test Device on Acoustic Emission Signals From Nuclear Safety Experiments: Contribution of Wave Propagation Modeling to Signal Processing. IEEE Transactions on Nuclear Science, 2018. 65(9): p. 2479-2489.
- [24] Brath, A.J., et al., Acoustic formulation of elastic guided wave propagation and scattering in curved tubular structures. IEEE transactions on ultrasonics, ferroelectrics, frequency control 2014. 61(5): p. 815-829.
- [25] IEEE Draft Guide for the Detection, L.a.I.o.S.o.A.E.f.E.D.i.P.T.a.P.R., in IEEE PC57.127/D3, October 2017 , vol., no., pp.1-65, 1 Jan. 2018.
- [26] Wotzka, D., T. Boczar, and P. Frącz, Mathematical model and numerical analysis of AE wave generated by partial discharges. Acta Physica Polonica A, 2011. 120(4): p. 767-771.
- [27] Ghosh, R., B. Chatterjee, and S. Dalai, A method for the localization of partial discharge sources using partial discharge pulse information from acoustic emissions. IEEE Transactions on Dielectrics Electrical Insulation 2017. 24(1): p. 237-245.
- [28] Wang, Y.-B., et al., Acoustic localization of partial discharge sources in power transformers using a particle-swarm-optimization-route-searching algorithm. IEEE Transactions on Dielectrics Electrical Insulation, 2017. 24(6): p. 3647-3656.
- [29] Hao, B., et al., A Study of the Properties of a Piezoelectric Ceramic Plate in the Symmetric Fixation Mode. IEEE Access, 2018. 6: p. 36863-36873.
- [30] Sobocinski, M., et al., A piezoelectric active mirror suspension system embedded into low-temperature cofired ceramic. IEEE Transactions on Ultrasonics, Ferroelectrics, and Frequency Control, 2012. 59(9): p. 1990-1995.
- [31] Zhu, M. and G. Leighton, Dimensional reduction study of piezoelectric ceramics constitutive equations from 3-D to 2-D and 1-D. IEEE Transactions on Ultrasonics, Ferroelectrics, and Frequency Control, 2008. 55(11): p. 2377-2383.
- [32] Li, J., et al., A Partial Discharge Detection Method for SF6 Insulated Inverted Current Transformers Adopting Inner Shield Case as UHF Sensor. IEEE Transactions on Power Delivery, 2018.
- [33] Boya, C., et al., Location of partial discharges sources by means of blind source separation of UHF signals. IEEE Transactions on Dielectrics Electrical Insulation 2015. 22(4): p. 2302-2310.
- [34] Wang, Y., et al., Research on a practical de-noising method and the characterization of partial discharge UHF signals. IEEE Transactions on Dielectrics Electrical Insulation, 2014. 21(5): p. 2206-2216.
- [35] IEEE Guide for the Electromagnetic Characterization of Conductive Gaskets in the Frequency Range of DC to 18 GHz. IEEE Std 1302-1998, 1998: p. i.
- [36] Hou, H., G. Sheng, and X. Jiang, Robust time delay estimation method for locating UHF signals of partial discharge in substation. IEEE Transactions on Power Delivery, 2013. 28(3): p. 1960-1968.
- [37] Catrysse, J., et al. A New Stripline Measuring Setup for the Characterisation of Conductive Gaskets up to 18GHz. in Proceedings of the International Symposium on Electromagnetic Compatibility. 2010.
- [38] Catrysse, J., et al. A Measuring Setup for the Characterization of in-circuit Conductive Gaskets up to 40 GHz. in Proceedings of EMC Europe 2012, Rome. 2012.
- [39] Du, J., et al., Investigation on the propagation characteristics of PD-induced electromagnetic waves in an actual 110 kV power transformer and its simulation results. IEEE Transactions on Dielectrics Electrical Insulation, 2018. 25(5): p. 1941-1948.
- [40] Itoh, T., Y. Hirokawa, and S. Ikuno, High-Performance Computing of Electromagnetic Wave Propagation Simulation Using Meshless Time-Domain Method on Many Integrated Core Architecture. IEEE Transactions on Magnetics, 2015. 51(3): p. 1-4.
- [41] Nishigouchi, K., et al., Waveform estimation of particle discharge currents in straight 154 kV GIS using electromagnetic wave propagation simulation. IEEE Transactions on Dielectrics and Electrical Insulation, 2013. 20(6): p. 2239-2245.
- [42] Takami, J., T. Tsuboi, and S. Okabe, Measured Distortion of Current Waves and Electrical Potentials With Propagation of a Spherical Wave in an Electromagnetic Field. IEEE

- Transactions on Electromagnetic Compatibility, 2010. 52(3): p. 753-756.
- [43] Duan, Y., et al., Present Situation and Prospect of Internal Sensors for UHF Detection in GIS. *Applied Mechanics Materials*, 2015.
- [44] Khaleghi, A., I. Balasingham, and A. Vosoogh. A compact ultra-wideband spiral helix antenna for in-body communications. in *Antennas and Propagation (EuCAP)*, 2014 8th European Conference on. 2014. IEEE.
- [45] Goksel, O., H. Eskandari, and S.E. Salcudean, Mesh adaptation for improving elasticity reconstruction using the FEM inverse problem. *IEEE transactions on medical imaging*, 2013. 32(2): p. 408-418.
- [46] Lamecki, A. and Techniques, A Mesh Deformation Technique Based on Solid Mechanics for Parametric Analysis of High-Frequency Devices With 3-D FEM. *IEEE Transactions on Microwave Theory*, 2016. 64(11): p. 3400-3408.
- [47] Silva, I. and G.B. Moody, An open-source toolbox for analysing and processing physionet databases in matlab and octave. *Journal of open research software*, 2014. 2(1).
- [48] Xia, H., et al., Noise Reduction Method for Acoustic Sensor Arrays in Underwater Noise. *IEEE Sensors Journal*, 2016. 16(24): p. 8972-8981.
- [49] Benesty, J., J. Chen, and Y. Huang, A Widely Linear Distortionless Filter for Single-Channel Noise Reduction. *IEEE Signal Processing Letters*, 2010. 17(5): p. 469-472.